The Effect of Proprioceptive Feedback on the Distribution of Sensory Information in a Model of an Undulating Organism

Ben Jones, Yaochu Jin, Bernhard Sendhoff, Xin Yao

2009

Preprint:

This is an accepted article published in 10th European Conference on Artificial Life. The final authenticated version is available online at: https://doi.org/[DOI not available]

The Effect of Proprioceptive Feedback on the Distribution of Sensory Information in a Model of an Undulating Organism

Ben Jones[1], Yaochu Jin[2], Bernhard Sendhoff[2], Xin Yao[1]

[1]School of Computer Science, The University of Birmingham, UK
[2]Honda Research Institute Europe GmbH, Germany

Abstract. In an animal, a crucial factor concerning the arrival of information at the sensors and subsequent transmission to the effectors, is how it is distributed. At the same time, higher animals also employ proprioceptive feedback so that the neural circuits have information regarding the state of the organism's body. In order to disseminate what this practically means for the distribution of sensory information, we have modeled a generic swimming organism (animat) coevolving its nervous system and body plan morphology. In a simulated aquatic environment, we find that animats artificially endowed with proprioceptive feedback are able to evolve completely decentralized central pattern generators (CPGs). Without such feedback however, we secondly find that the distribution of sensory information from the head of the animat becomes far more important, with adjacent CPG circuits becoming interconnected. Crucially, this demonstrates that where proprioceptive mechanisms are lacking, more effective delivery of sensory input is essential.

1 Introduction

The state of a given animal's external environment or niche, is presented to the animal via its sensory system. This generates informational cues regarding for example, predator or prey items, allowing the animal's nervous system to invoke either pervasive or evasive behaviours. Typically over time, the animal is able to learn and adapt[1]. Higher animals also employ proprioceptive mechanisms enabling them to detect the current state of the locomoting body, serving as a sensory feedback mechanism for the underlying neural circuit. Previous studies have shown that central pattern generators (CPGs) responsible for the periodic movement control are all affected and constrained by such feedback, e.g. [13]. Other studies have highlighted how feedback can help undulatory organisms surpass a 'speed barrier', [7,8]. The necessity of proprioception in the peristaltic movements of drosophila larvae has also been established, without which, locomotion is seen to be significantly degraded, [16]. Typically such proprioceptive mechanisms are 'stretch receptors' within the animal's exoskeleton, e.g. [6]. In order for the animal to respond correctly, all of this sensory information has to reach the appropriate effectors.

[1] Note that in this paper, we have no concept of learning, rather behaviour is considered only in reactive 'braitenberg vehicle' terms, [4].

We pick up on the point of proprioceptive feedback and its influence on sensory information distribution. We model a segmented three dimensional aquatic organism with movement mechanisms not dissimilar to the vertebrate lamprey. In an initial experiment, the animat is endowed with a proprioceptive mechanism whilst in the second, it is not. In both, the animat has an abstract visual system which it may or may not utilise depending on how the neural circuits become interconnected. The goal is for the animat to swim forwards towards a predefined target.

Whilst the field of physically realistic locomotion is old (see [9] for a review), the incorporation of some abstract visual system is novel. Beauregard and Kennedy model a 2D lamprey able to undertake tracking of a moving object, [2]. Indeed, the visual system that their model utilises provides a basis in our model. Ijspeert models a visual system in a 3D simulated salamander able to track a moving object both in land and water, [10]. In Biology, Deliagina et al. have found activity differences in the reticulospinal neurons, a system within the lamprey transmitting signals from the brain to the spinal cord, whenever the lamprey turns, [5]. This highlights the functional significance of effective information distribution from sensors to effectors. The rest of this paper is laid out as follows. Section 2 gives an overview of the simulation environment. Section 2.3 provides experimental details. Section 3 presents our main findings. We conclude in Section 4.

2 Simulation Environment

The simulation environment has been implemented in C++. There are 2 main components making up the system: the animat and the evolutionary setup. They are explained below and an overview of the experimental setup also follows.

2.1 Animat

Geometry The animat is soft-bodied being entirely constructed out of springs. These springs are connected together to form cuboids which are then themselves connected together to form the overall morphology, Fig. 1a.

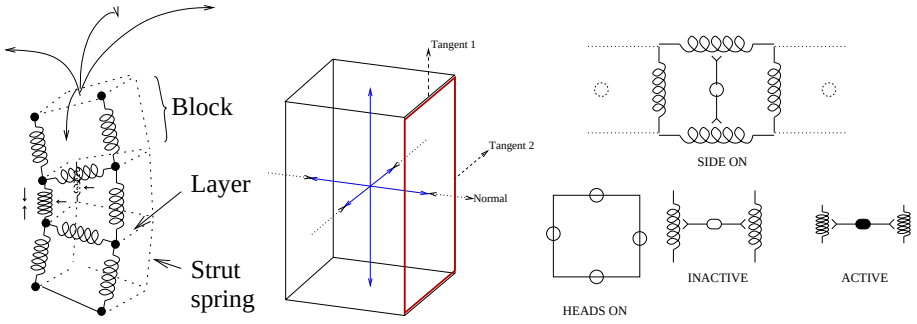

(a) Animat construction (b) Compass system. (c) Motor system

Fig. 1: Animat geometry. The compass system is used to derive water forces.

The water force model An external water force is applied to each face of a given animat block. The force is derived from the velocity of the face which is taken to be the average velocity of all four point masses, similar to, e.g. [15]. The force is computed by initially splitting the velocity vector into its three components (as highlighted in Fig. 1b):

$$t_1 = \hat{\mathbf{t_1}} \cdot \mathbf{v} \qquad t_2 = \hat{\mathbf{t_2}} \cdot \mathbf{v} \qquad n = \hat{\mathbf{n}} \cdot \mathbf{v} \tag{1}$$

where $\hat{\mathbf{t_1}}$, $\hat{\mathbf{t_2}}$ and $\hat{\mathbf{n}}$ are normalised tangent and vector components of the block face and $\mathbf{v}$ is the velocity of the face. We then compute the three force components as follows:

$$\Xi(t_1) = -\gamma_{t_1} \text{sgn}(t_1)(t_1)^2 \tag{2}$$

$$\Xi(t_2) = -\gamma_{t_2} \text{sgn}(t_2)(t_2)^2 \tag{3}$$

$$\Xi(n) = -\gamma_n \text{sgn}(n) n^2 \tag{4}$$

where the γ parameters control the levels of application of each of the three components. The actual water force, $\mathbf{w}$, that can be applied to each of the four point masses making up the block face is calculated as follows:

$$\mathbf{f} = \Xi(t_1)\hat{\mathbf{t_1}} + \Xi(t_2)\hat{\mathbf{t_2}} + \Xi(n)\hat{\mathbf{n}} \tag{5}$$

$$\mathbf{w} = \mathbf{f} c d A \tag{6}$$

where c is a viscosity coefficient, d is drag and A is the area of the block face. Note that in our model we have set c and d to 1 since it is sufficient to tune the γ parameters.

Neural system The neural system is based on a continuous time recurrent neural network. The membrane potential, u_j, of a neuron is modelled as follows, [3]:

$$\frac{du_j}{dt} = \frac{1}{\tau_j}\left(-u_j + \sum_{i=1}^{C} w_{ji} a_i + I_j\right) \tag{7}$$

where τ_j is a time constant, w is a vector of presynaptic connection weights and I_j is an external input current. The value a_i is a presynaptic neuron's membrane activity computed as follows:

$$a_i = \begin{cases} \tanh(u_i - \beta_i) & |u_i| > 0 \\ 0 & \text{otherwise} \end{cases} \tag{8}$$

Note that given Eq. 8, the function is only employed if the neuron's membrane potential is not 0. We have this restriction in order to ensure that neurons need some initial input, for example, from a sensor, before they can generate any kind of dynamic. Without it, a neuron would always potentially have an activity, because the bias value, β_j, would allow for this. The weight values are computed from the interneuronal Euclidean distance as in [11,12]. Connectivity also comes about as a function of distance according to the sigmoid,

$$\sigma(\lambda, s, d_{ij}) = \frac{2}{2 + \exp((\lambda/s) * d_{ij})} \tag{9}$$

where λ is an evolved parameter, s is a scaling parameter set to 4.5 and d_{ij} is the Euclidean distance between neurons *i* and *j*. A connection is established if the function produces a value >0.5.

Motor system Each motor is an excitatory neuron. Being position-fixed, it is also considered part of the body plan. Each animat block has 4 motors, 1 associated with each face of the block. A given motor actuates a vertical spring-pair of the block face, see Fig. 1c. The amount of force applied to each spring is proportional to the membrane potential of the associated motor neuron.

Sensory system The animat has a very rudimentary sensory system consisting of 4 sensory neurons that remain position-fixed at the head of the animat (one at the top-middle of each block face). Current is injected only into the closest sensor from the target and is inversely proportional to the angle of the target from the given sensor. Whilst there are no turning constraints required in our later experiments, this setup paves the way for future experimentation. The input current injected into the closest sensory cell is thus: $I_s = \exp(\phi + 0.01)$.The value 0.01 ensures that there will be some input current, even when the target angle, ϕ, is 0. Note that this sensory mechanism is partially based on the exponentiated bearing-based tracking model employed in [2].

Proprioceptive feedback mechanism The proprioceptive mechanism is based on a notion of stretch receptor activity, for example, that found in the leech, [6]. Also, as with the sensory system outlined above, the proprioceptive mechanism is exponentiated taking the amount of side spring distension as input (difference in length of spring from resting length). This input current, I_M, is then fed directly into the associated motor neuron computed as $I_M = \exp(\Delta d)$ where Δd is the level of spring distension.

2.2 Evolved Components

A mixed real-valued and Boolean evolutionary algorithm having discrete recombination, self-adaptive mutation (see [1]) and tournament selection with an elitist strategy is used to evolve a genotype consisting of three main components: the body-plan, the neural architecture, and the neural properties.

Body-plan In the simulation, we consider the number of body segments, the length of each segment and the symmetry of the active motor configuration (refer to [11] for details of this latter aspect) to all be parts of the body-plan morphology. Note also that when the length of a segment changes, the neural distribution's spread within that segment commensurately changes.

Neural architecture Inside of each body plan segment, there are 6 interneurons, the polar coordinate positions of which are randomly initialised and subsequently evolved. Secondly, a set of λ values tuning the connectivity function as given in Eq. 9 are also evolved depending on the type of connectivity: λ_{II}, λ_{IE}, λ_{SE}, λ_{AA} where I=interneuron, E=effector neuron, S=sensory neuron; AA indicates connections between interneurons in adjacent segments.

Neural properties These include the neuron time-constants, thresholds and whether or not a neuron is inhibitory. A weight value between a neuron pair is derived according to the distance between them, as in [11,12].

2.3 Experimental overview

Our experiments address how sensory information should be distributed when we consider proprioceptive mechanisms, especially in view of connectivity patterns that might

emerge between different neural circuits. We have therefore conducted two sets of 30 experiments for statistical significance with each individual experiment being allowed to run for 500 generations. In the first setup, the animat is endowed with proprioceptive feedback. In the second, it is not. In both, the animat is required to swim forwards in order to reach a pre-defined target. The fitness function is simply $f_1 = 20.0 - d_{target,animat}$, see Fig. 2.

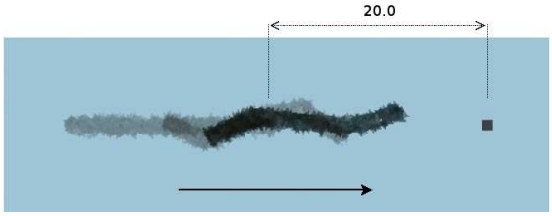

Fig. 2: A sequence of overlaid screenshots at behavioural iterations 1, 245 and 384 (a total of 400 are permitted) for an evolved animat. The animat's task is to swim towards the cube in the direction indicated by the lower arrow.

3 Results

In Fig. 3, we can see that animats endowed with the proprioceptive mechanism performed significantly better than those that were not. We can secondly observe, that a higher number of connections were required in those animats without the proprioceptive mechanism. A higher number of connections equates to connections forming between neurons in adjacent neural circuits and some connections for the sensory neurons located in the head of the animat. Representative neural architectures depicting two such animats are given in Fig. 4. Finally, we relate such architectural distribution to total wire length and total number of neuronal oscillations observing that for the animats without proprioceptive feedback, there is a marked increase in total wire length, see the left panel of Fig. 5. This is to be expected since the neural circuits in adjacent segments become connected resulting in more wire. We secondly find that animats without proprioceptive mechanisms generate a higher number of neuronal oscillations, refer to the right panel of Fig. 5.

Although it would appear that proprioception as it exists in our model benefits the animat behaviour, it is difficult to know with any certainty whether the feedback mechanism is truly serving to modulate the neuronal dynamics as would be the case in true proprioception, or, whether it is just triggering the network to reach a particular attractor state. In order to test this, we have performed a final set of experiments taking the 30 best proprioceptive individuals and replacing the feedback mechanism with varying levels of noise. As mentioned in the model description (subsection 2.1), this feedback mechanism works by injecting into an associated motor neuron, an input current that is proportional to the level of spring distension. Replacing it with a uniform noise simply substitutes the input current for a float value generated from the range [-n,n]. The smallest level of noise chosen was [-0.2,0.2], whilst the largest was [-2,2]. If the feedback is only serving to trigger the network then we can expect the animat to be robust to arbitrary value. The results are presented in Fig. 6. We can see that up to a noise

range of [-1.2,1.2] the performance is slightly degraded but all performances up to this point are approximately equal, whilst a noise range greater or equal to [-1.4,1.4] sees a degradation in animat performance.

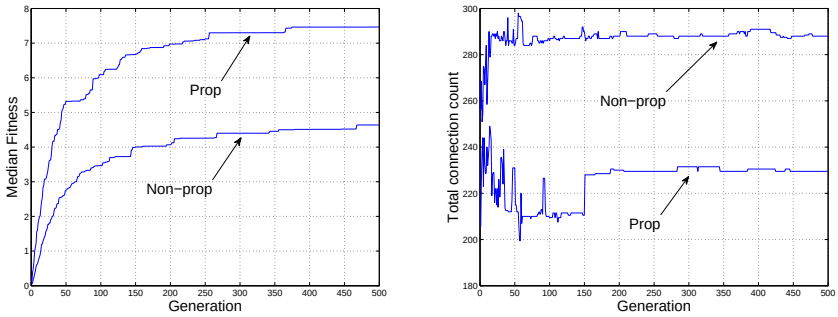

Fig. 3: Comparison of fitness medians and connectivity count medians for proprioceptive and non-proprioceptive variants

4 Conclusion

Since proprioceptive animats performed better, we can conclude that proprioception advances the animat's ability to locomote forwards. Furthermore, given the results in which we removed the true proprioception and replaced it with noise, it is likely that up to a point, the feedback is serving as a trigger mechanism since the undulatory behaviour is seen to be robust with a slight performance degradation (from [-0.2,0.2] to [-1.2,1.2]). However if the noise is advanced to too great a level (from [-1.4,1.4] to [-2.0,2.0]), performance is seen to be degraded indicating two things. Firstly, that the system is not robust to high levels of noise, and secondly, that correct proprioceptive feedback has a fitness enhancing if not modulating effect on the neural dynamics since in actual fact, any level noise is seen to degrade the performance.

Interestingly, when the animat is endowed with a feedback mechanism, the neural architecture evolves to become completely decentralised with regards to the individual neural circuits. This is a response to evolutionary pressure since connections could have evolved between the neural circuits if there had been any selective advantage. A fully decentralized architecture inferably necessitates a reduction in interference between the neural circuits thus ensuring correct oscillatory dynamics. Indeed, by artificially adding interconnections, the performance of such an animat is degraded (results not shown). Therefore in some cases, centralized control, or at least some interconnectivity between individual CPG 'modules', can be detrimental.

Thirdly, since in the non-proprioceptive variant there were no feedback mechanisms, the neurons could not directly rely on body-shape information. In the proprioceptive case however, the actual body was allowed to become part of the dynamic coupling existing between the behaving body and underlying neural system. Therefore, with regard to the number of neuronal oscillations in Fig. 5, we can plausibly speculate that in the proprioceptive case, much of the oscillatory dynamic could be offloaded

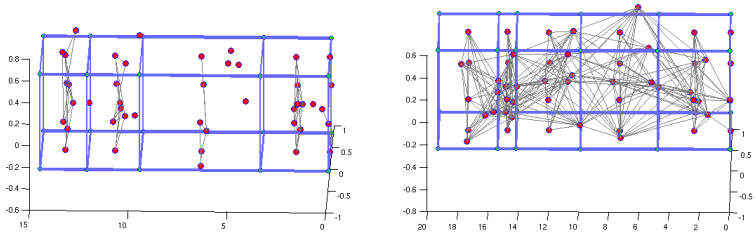

(a) Proprioceptive (b) Non-proprioceptive

Fig. 4: Representative architectures to have evolved for each setup. For the proprioceptive individual, the architecture is seen to be decentralized, with no connections between the individual neural circuits. By contrast, such connections do exist in the non-proprioceptive individual.

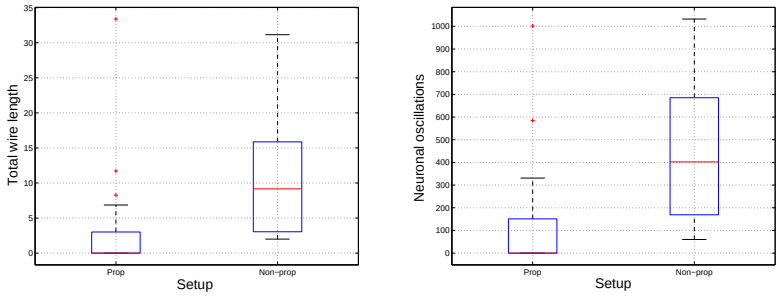

Fig. 5: Box plots of best wire lengths and neural oscillations, highlighting firstly a larger wire length for the non-proprioceptive individuals; secondly, a larger number of neuronal oscillations for the non-proprioceptive individuals.

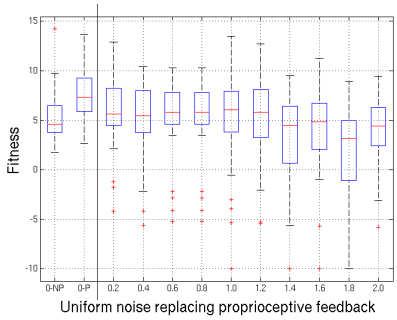

Fig. 6: A boxplot showing how differing amounts of uniform noise used to replace the proprioceptive feedback mechanism, affects fitness. The ‘0-NP’ and ‘0-P’ cases left of the vertical line are the non-proprioceptive and proprioceptive plots without any such noise whilst those to the right are the proprioceptive individuals with noise replacing the feedback.

to the oscillating body and that this enabled a reduction in the number of neuronal oscillations or 'computational effort' of the neural system. This is a nice example of morphological computation, [14].

There are a number of major extensions that we envisage. The first involves analysis of the different body plan components, for example body plan segment length and number of body-plan segments, in terms of how they effect the performance of the animat. Work has begun on this. The second major undertaking will incorporate an energy measure as we did for a model of a radially symmetric organism in [12]. Finally, we might incorporate a developmental process into the model so that it more realistically reflects biological systems.

References

1. T. Bäck and H.-P. Schwefel. An overview of evolutionary algorithms for parameter optimization. *Evolutionary Computation*, 1(1):1–23, 1993.
2. M. Beauregard and P.J. Kennedy. Robust simulation of lamprey tracking. In *Parallel Problem Solving from Nature - PPSN IX*, pages 641–650, Berlin, 2006. Springer-Verlag.
3. J. Blynel and D. Floreano. Levels of dynamics and adaptive behavior in evolutionary neural controllers. In *From Animals to Animats 7: Proceedings of the seventh international conference on simulation of adaptive behavior*. MIT Press, 2002.
4. V. Braitenberg. *Vehicles, Experiments in Synthetic Psychology*. Cambridge, Mass, 1984.
5. T.G. Deliagina, V. Zelenin, P. Fagerstedt, S. Grillner, and G.N. Orlovsky. Activity of reticulospinal neurons during locomotion in the freely behaving lamprey. *Journal of Neurophysiology*, 83:853–863, 2000.
6. W.O. Friesen and W.B. Kristan. Leech locomotion: swimming, crawling, and decisions. *Neurobiology of Behaviour*, 17:704–711, 2008.
7. S. Grillner, A. Kozlov, P. Dario, and C. Stefanini. Modeling a vertebrate motor system: pattern generation, steering and control of body orientation. *Progress in Brain Research*, 165, 2007.
8. A. J. Ijspeert, J. Hollam, and D. Willshaw. Evolving swimming controllers for a simulated lamprey with inspiration from neurobiology. *Adaptive Behavior*, 7(2):151–172, 1999.
9. A.J. Ijspeert. Central pattern generators for locomotion control in animals and robots. *Neural Networks*, 21(4):642–653, 2008.
10. A.J. Ijspeert and M. Arbib. Visual tracking in simulated salamander locomotion. In *Sixth International Conference of The Society for Adaptive Behavior (SAB2000)*, pages 88–97, Paris, 2000.
11. B. Jones, Y. Jin, B. Sendhoff, and X. Yao. Evolving functional symmetry in a three dimensional model of an elongated organism. In *Proceedings, ALife XI*, pages 305–312, Winchester, UK, 2008.
12. B. Jones, Y. Jin, X. Yao, and B. Sendhoff. Evolution of neural organization in a hydra-like animat. In *ICONIP Conference Proceedings*, Auckland, 2008. Springer.
13. J. Nishii. A learning model of a periodic locomotor pattern by the central pattern generator. *Adaptive Behavior*, 7(2):137–149, 1999.
14. R. Pfeifer and F. Iida. Morphological computation: Connecting brain, body, and environment. In *Lecture Notes in Computer Science*, volume 3853. Springer, 2006.
15. M. Sfakiotakis and D.P. Tsakiris. Simuun: A simulation environment for undulatory locomotion. *International Journal of Modelling and Simulation*, 2006.
16. W. Song, M. Onishi, L. Y. Jan, and Y. N. Jan. Peripheral multidendritic sensory neurons are necessary for rythmic locomotion behaviour in drosophila larvae. *PNAS*, 104(12):5199–5204, 2007.